



Efficient and sustainable tandem annulation-decarboxylation reaction using ecocatalysis

Laure Liénart, Yves-Marie Legrand, Franck Pelissier, Philippe Gaveau, Peter Hesemann, Eddy Petit, Claude Grison, Claire Grison

► To cite this version:

Laure Liénart, Yves-Marie Legrand, Franck Pelissier, Philippe Gaveau, Peter Hesemann, et al.. Efficient and sustainable tandem annulation-decarboxylation reaction using ecocatalysis. *Applied Catalysis B: Environmental*, 2024, 349, pp.123888. 10.1016/j.apcatb.2024.123888 . hal-04488807

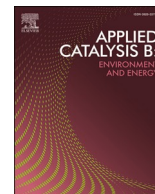
HAL Id: hal-04488807

<https://hal.science/hal-04488807>

Submitted on 4 Jul 2024

HAL is a multi-disciplinary open access archive for the deposit and dissemination of scientific research documents, whether they are published or not. The documents may come from teaching and research institutions in France or abroad, or from public or private research centers.

L'archive ouverte pluridisciplinaire **HAL**, est destinée au dépôt et à la diffusion de documents scientifiques de niveau recherche, publiés ou non, émanant des établissements d'enseignement et de recherche français ou étrangers, des laboratoires publics ou privés.



Efficient and sustainable tandem annulation-decarboxylation reaction using ecocatalysis

Laure Liénart^a, Yves-Marie Legrand^a, Franck Pelissier^a, Philippe Gaveau^b, Peter Hesemann^b, Eddy Petit^c, Claude Grison^{a,*}, Claire M. Grison^{a,*}

^a ChimEco, Univ Montpellier, CNRS UMR 5021, Montpellier, France

^b ICGM, Univ Montpellier, CNRS UMR 5253, ENSCM, Montpellier, France

^c IEM, Univ Montpellier, CNRS UMR 5635, ENSCM, Montpellier, France

ARTICLE INFO

Keywords:

Substituted cyclohexenone
Tandem reaction
Green metrics
Environmental catalysts
Biomass wastes

ABSTRACT

Substituted cyclohexenones are well-known building blocks for the synthesis of numerous natural products and bioactive compounds. Despite their widespread use, they are prepared under conditions that are not compatible with the principles of green chemistry. Here the synthesis of substituted cyclohexenones was revisited using a tandem annulation-decarboxylation strategy, in an eco-friendly process without compromising on efficiency. To meet this challenge, environmental catalysts, named ecocatalysts®, which derived from biomass wastes were used. Under microwave activation, ecocatalysis assisted by statistical tools led to excellent yields, as well as remarkable green metrics for the whole synthetic process, which both exceeded those previously reported. The reaction was scaled-up allowing the recycling assessment of the best ecocatalysts®. The reaction was also extended to other substrates. The catalytically active species within the best ecocatalyst® was identified through extensive characterisation by MP-AES, XRPD, SEM, XPS and solid-state NMR, allowing to depict a mechanism confirmed by DFT calculations.

1. Introduction

Cyclohexenones have been widely used as building blocks for the synthesis of more complex natural or biologically active compounds with anticancer, antimicrobial, antiviral, antineurodegenerative, immunomodulatory, contraceptive or pheromone-like properties [1,2]. They have also been employed in conjugation chemistry leading to medicinally interesting derivatives [3]. In both cases, cyclohexenones could be derivatised by several reactions, as cycloaddition reactions [4], 1,4-additions [5,6], 1,2-additions [7], 2-halogenations [8] or Pd (II)-catalysed enantioselective arylboronic acid additions [9,10]. Despite their widespread use, most syntheses of substituted cyclohexenones are indirect and require several steps leading to low or moderate overall yields. For example, the synthesis of 3-methyl-2-cyclohexenone, or seudenone, an insect pheromone isolated from the destructive pest *Dendroctonus pseudotsugae*, was reported in 2–3 steps with a yield range of 50–60%, according to the strategy, the Birch reduction of 3-methylanisole [11,12], the Wittig reactions of δ -keto-carboxylic acids [13] and the oxidation of 1,8-cineole followed by a

retro-aldol condensation [14]. Inspired from an annulation approach using acyclic precursors, a tandem annulation-decarboxylation synthesis was reported as an alternative single-step strategy and with better yields [15–17]. However, the reaction conditions were not compatible with the principles of green chemistry as petroleum-based strong bases, long reaction time and waste-producing workup were needed.

Here, the synthesis of substituted cyclohexenones was revisited using the same tandem annulation-decarboxylation strategy in an environmentally friendly process while intending to improve the yields previously reported. Environmental catalysts, named ecocatalysts® [18–24], which derived from biomass wastes were used to replace the usual petrochemical bases. Two types of biomasses were selected: food waste as spent coffee ground and plants that are problematic for the biodiversity and require their removal from the environment as Invasive Alien Species (IAS) (*Fallopia japonica* and *Arundo donax*) [25] and as fast-growing species (*Salix alba*). Indeed, the management of such biomasses is costly and developing an alternative utilisation of the derived wastes represents an economic support [18,26].

In addition to being environmental wastes, the biomasses must bear

* Corresponding authors.

E-mail addresses: claudio.grison@cnrs.fr (C. Grison), claire.grison.2@cnrs.fr (C.M. Grison).

<https://doi.org/10.1016/j.apcatb.2024.123888>

Received 30 November 2023; Received in revised form 20 February 2024; Accepted 26 February 2024

Available online 28 February 2024

0926-3373/© 2024 Published by Elsevier B.V.

two main criteria: being abundant and displaying a high content in K and/or Mg related to potential Brønsted basic and/or Lewis acidic properties [20,27]. Indeed, ecocatalysts® derived from *F. japonica* and *S. alba* to a lesser extent catalysed the Michael addition of dimethylmalonate onto 2-alkyl cyclopentenones illustrating their basic activities [27].

Extending these results, ecocatalysts® derived from *F. japonica*, *A. donax*, *S. alba* and spent *Coffea arabica* were prepared and analysed by MP-AES and XRPD. They were engaged in the model reaction for the synthesis of 3-methyl-2-cyclohexenone under microwave activation. Using Spearman correlations, the reaction conditions were optimised with the four ecocatalysts® and the influence of the key experimental factors were detailed. Recycling and reuse of the best ecocatalyst® were studied, allowing the calculation and comparison to literature of seven green metrics of the model reaction process. The reaction was then extended to other mono- and disubstituted cyclohexenones. Finally, a fine study of the catalytically active species within the best ecocatalyst® was performed by comparing its reactivity versus commercial salts and by a deeper characterisation by SEM, XPS and solid-state NMR. The reaction mechanism was revisited with the catalytically active species supported by DFT calculations.

2. Experimental part

2.1. Materials

3-buten-2-one (90%), 1-penten-3-one (97%), crotonaldehyde (99.5%), glycerol (>99%), $\text{Ca}_5(\text{PO}_4)_3\text{OH}$ and MgO were purchased from Sigma-Aldrich. Methacrolein (90%), mesityl oxide (95%), ethyl acetoacetate (98%), ethyl 2-methylacetoacetate (95%) and ethyl 3-oxovalerate (97%) were purchased from TCI. 3-penten-2-one (85%) was purchased from Alfa Aesar. CaCO_3 was purchased from Carlo Erba Reagents. Pure Arabica coffee grounds were purchased from Carte Noire.

2.2. Methods

2.2.1. Analysis and quantification

2.2.1.1. MP-AES analysis. The elementary composition of ecocatalysts® was measured using an Agilent MPAES4210 Microwave Plasma Atomic Emission Spectroscopy with an Agilent SPS 3 Autosampler. We used dinitrogen supplied via an F-DGSI N2 generator Thyster 1Df for the plasma. The samples were introduced via a OneNeb nebulizer and a single-pass cyclonic spray chamber. All samples were prepared by microwave digestion using an Anton Paar Multiwave Go. A mixture of HNO_3 (4 mL, 65%) and HCl (2 mL, 37%) was added to the ecocatalyst® material (100 mg), using a method specially developed for the samples (20 min ramp to 164 °C and 10 min at 164 °C). Once cooled, the solutions were diluted to 50 mL with ultrapure water with 1% of HNO_3 and diluted 10 times before injections.

2.2.1.2. Quantification by GC-MS and GC-FID. Gas chromatography analyses were performed using a Thermo Scientific Trace 1300 device with dihydrogen as the vector gas coupled with an ISQ simple quadrupole mass detector for the identification and FID flame ionisation detector was used for quantification. The column was a Trace TR-5MS column 30 m, 25 mm, 25 μm Thermo Scientific.

In brief, 1 μL of solution was introduced into the GC-MS-FID with an injector temperature of 280 °C; split mode was 1/20 with a flow gas of 1 mL/min. The column temperature was programmed as follows: initially, the temperature was kept at 40 °C for 1 min and then heated up to 280 °C with a rate of 70 °C/min and held at 280 °C for 2 min. The run time was 7 min.

The mass spectra of products were recorded using Electron Ionisation in positive ion mode. The transfer temperature was 300 °C. A full scan

mode ($m/z = 50\text{--}650$) was used with centroid acquisition. Scan time was 0.05 s.

An air flow of 350 mL/min, a dihydrogen flow of 33 mL/min was used for the FID and the detector temperature was 280 °C.

The quantification of the molecule concentration was monitored by GC-FID using external calibration.

2.2.1.3. Nitrogen sorption isotherms. Nitrogen sorption isotherms were recorded at 77 K on a Micromeritics TriStar volumetric apparatus by admitting doses of nitrogen in a measurement cell. Prior to the nitrogen sorption experiments, the samples were outgassed at 200 °C under vacuum overnight. The BET surface area of each sample was determined using the Brunauer-Emmett-Teller (BET) method [46] on the linear range of the isotherms typically at $p/p^0 = 0.05\text{--}0.35$.

2.2.1.4. Scanning electron microscopy (SEM). SEM images were recorded on a Zeiss EVO HD15 Scanning Electron Microscope.

2.2.1.5. X-ray powder diffraction (XRPD) analysis. XRPD data measurements were performed using a Bruker diffractometer (D8 Advance, with a $\text{Cu K}\alpha$ radiation $\lambda = 1.54086 \text{ \AA}$) equipped with a Lynxeye detector.

2.2.1.6. X-ray photoelectron spectrometry (XPS) analysis. XPS measurements were performed (ESCALAB 250 from Thermo Electron) on commercial MgO and on Eco1-E-spent *C. arabica* with a monochromatic excitation source, Al $\text{K}\alpha$ x-rays (1486.6 eV) operating at 15 kV and 6 mA. A spot size of 500 μm , a transition energy of 150 eV at a step of 1 eV for the survey and a transition energy of 20 eV at step of 0.1 eV for high-resolution were used. The photoelectron spectra were calibrated using the binding energy of C=C component of C1s at 284.4 eV.

2.2.1.7. Analysis by ^1H and ^{13}C NMR. ^1H and ^{13}C solution NMR spectra were recorded on an Avance III Bruker 600 MHz spectrometer equipped with a TCI Prodigy cryoprobe.

2.2.1.8. Analysis by ^{25}Mg solid-state NMR. ^{25}Mg solid-state NMR experiments were performed on Eco1-E-spent *C. arabica* and commercial MgO dilute at the same wt% of Mg (8.1% in average) of the ecocatalyst®. The experiments were conducted on a VARIAN VNMRs 600 MHz spectrometer (PT-ICGM France) using a 7.5 mm HX probe. Samples were spun at 5 kHz at room temperature. Spectra were recorded using a single pulse sequence with a $\pi/2$ quadrupolar solid pulse of 3 μs and a relaxation delay D1 of 100 s (to accommodate the long relaxation time of MgO). The number of transients acquired was 822 for Eco1-E-spent *C. arabica* and 188 for commercial MgO dilute at 8% in Al_2O_3 . ^{25}Mg NMR chemical shifts were referenced a 1 mol/L MgCl_2 aqueous solution ($\delta = 0 \text{ ppm}$).

2.2.2. Synthesis

2.2.2.1. Harvest and collection of ecocatalysts®. Spent coffee grounds were collected from the wasted coffee grounds after preparation of pure Arabica coffee in our laboratory. Spent coffee grounds were collected at different period of time (January, July and October 2023), coming from different batches of the same producer (Carte Noire).

Leaves of *Salix alba* were harvested in September and November 2022, and June 2023, in Picardie (France). The organic reactions were conducted using *S. alba*, which was harvested in June 2023.

Aerial parts (leaves, stems and petioles) of *Fallopia japonica* were harvested in June and September 2023, in Saint-Julien-de-la-Nef (France) by the BIOINSPIR company. The organic reactions were conducted using *F. japonica*, which was harvested in September 2023.

Aerial parts (leaves and stems) of *Arundo donax* were harvested in May 2022 and July 2023, at the Biopole of Grabels (France). The organic reactions were conducted using *A. donax*, which was harvested in May

2022.

2.2.2.2. Preparation of ecocatalysts®. After collection, aerial parts of *A. donax*, *F. japonica* and *S. alba* were ground and thermally treated in a furnace under air flow at 550 °C for 4 h generating Eco1-E-A. *donax*, Eco1-E-F. *japonica*, and Eco1-E-S. *alba* (with a granulometry of 500 – <50 µm, 50 – <50 µm and 100 – <50 µm). Spent coffee grounds were thermally treated in a furnace under air flow at 550 °C for 4 h generating Eco1-E-spent *C. arabica*. The granulometry of Eco1-E-spent *C. arabica* was <50 µm. The resulting ashes were directly used as catalysts.

In the name “Eco1-E”, the number “1” stands for the single thermal treatment in comparison to other ecocatalysts® that had been prepared following more complex procedures. The letter “E” stands for elements, meaning that the biomass from which the ecocatalyst® derives has not accumulated any specific element related to an associated phyto-technology, in comparison to other ecocatalysts® which could be enriched in trace metals.

Procedure for the model reaction: the synthesis of 3-methyl-2-cyclohexenone **3** with optimised conditions.

Ethyl acetoacetate (30 mmol, 3.83 mL, 2 equiv.), Eco1-E-spent *C. arabica* (0.17 mmol, 53 mg, 0.01 equiv. of Mg), 3-buten-2-one (15 mmol, 1.39 mL, 1 equiv.; purity = 90%) and glycerol (7.5 mmol, 0.6 mL, 0.5 equiv.) were mixed in a microwave reactor (CEM Discover® 2.0). The reaction mixture was ramped to temperature for 10 min until 220 °C, then was stirred for 45 min at 220 °C. After cooling to room temperature, the ecocatalyst® was filtered through sinter with ethyl acetate (10 mL) and the collected solution was concentrated under reduced pressure. The crude product was purified by flash-chromatography (cyclohexane/ethyl acetate: 90/10) providing 3-methyl-2-cyclohexen-1-one **3** in 90% yield as a light-yellow liquid.

2.2.2.3. General procedure for the recycling of Eco1-E-spent *C. arabica*. The reaction was carried out in twelve 75 mL microwave reactors working in parallel (CEM MARS 6™ Synthesis). In one reactor, ethyl acetoacetate (90 mmol, 11.5 mL, 1.5 equiv.), Eco1-E-spent *C. arabica* (0.66 mmol, 208 mg, 0.01 equiv.), 3-buten-2-one (60 mmol, 5.43 mL, 1 equiv.; purity = 90%) and glycerol (30 mmol, 2.2 mL, 0.5 equiv.) were mixed. Reaction mixtures were ramped to temperature for 20 min until 220 °C, then were stirred at 220 °C for 1 h. The crude product was purified by distillation and provided 3-methyl-2-cyclohexen-1-one **3** as a light-yellow liquid. The remaining solid was thermally treated in a furnace under air flow at 550 °C for 4 h and reused as such in the following run of reaction. Recycling was performed up to 3 runs.

2.2.2.4. General procedure for the scope of substituted cyclohexenones. On a 30 mmol scale reaction, β -keto ester (2 equiv.), Eco1-E-spent *C. arabica* (0.01 equiv. of Mg), conjugated enone (or enal) (1 equiv.) and glycerol (0.5 equiv.) were mixed in a microwave reactor (CEM Discover® 2.0). The reaction mixture was ramped to temperature for 10 minutes until 180 °C or 220 °C, then was stirred for 30–60 minutes at 180 °C or 220 °C. The crude product was quantified by GC-FID or NMR with mesitylene as internal standard. The product was further isolated by distillation (see ESI for details).

2.2.2.5. Statistical analysis of the reaction conditions. The exploration of the best reaction conditions was investigated by calculating a Spearman correlation matrix. The correlations were calculated from a total of 38 experiments performed with the four ecocatalysts® (Eco1-E-F. *japonica*, Eco1-E-A. *donax*, Eco1-E-S. *alba*, Eco1-E-spent *C. arabica*) and a total of 11 variables (the catalytic loading and its composition in Ca, K, Mg and Na, the thermal treatment of the ecocatalyst®, the quantity of glycerol, the reaction time, the reaction temperature and the yield). The significance of the correlation coefficients between the variables and the yield were evaluated by calculating p-Values using a t-test. p-Values lower than 0.05 were considered to reject the null hypothesis.

2.2.2.6. DFT calculations. Density Functional Theory (DFT) calculations were performed as implemented by Gaussian 16 C.01. The SCF convergence default was used for Gaussian and the symmetry constraint was ignored. A hybrid functional, which include a mixture of Hartree-Fock exchange with DFT exchange-correlation, was used. The PBE1PBE functional that uses 25% exchange and 75% correlation weighting, is known in the literature as PBE0. The 1996 pure functional of Perdew, Burke and Ernzerhof was made into a hybrid by Adamo [28]. The double- ζ basis set def2-SVP [29], with polarisation functions was used. The D3 version of Grimme dispersion with Becke-Johnson damping was added for empirical dispersion [30], typically used for non-covalent interactions, supramolecular complexes in solution.

3. Results

3.1. Structural characterisation of ecocatalysts®

Four ecocatalysts® were prepared by thermally treating in air biomass wastes coming from IAS, fast-growing species and spent coffee grounds generating Eco1-E-A. *donax*, Eco1-E-F. *japonica*, Eco1-E-S. *alba* and Eco1-E-spent *C. arabica*.

The elemental composition of ecocatalysts® was characterised by MP-AES (Fig. 1(a) & Table S1). All ecocatalysts® displayed the presence of physiological elements, Ca, K, Mg and Na, due to their biological origin but their concentration slightly differed from each other. Indeed, ecocatalysts® derived from IAS, Eco1-E-A. *donax* and Eco1-E-F. *japonica*, showed a high concentration of K while Eco1-E-S. *alba* and Eco1-E-spent *C. arabica* displayed well-distributed concentrations of elements.

The structure of ecocatalysts® was characterised by XRPD (see full spectra in Fig S1) and crystalline species were classified according to increasing pKa (Fig. 1(b)). All ecocatalysts® showed the presence of basic species such as magnesium oxide (periclase), carbonates (K_2CO_3 , fairchildite ($K_2Ca(CO_3)_2$), $CaCO_3$), and/or phosphates (hydroxyapatite ($Ca_5(PO_4)_3OH$)), but also the presence of other slightly acidic or neutral salts related to their natural origin.

3.2. Synthesis of 3-methyl-2-cyclohexenone **3**

3.2.1. Optimisation of the reaction conditions supported by statistical calculations

Considering the presence of basic species within the four ecocatalysts®, all ecocatalysts® were tested in the tandem annulation-decarboxylation reaction of β -ketoesters. The preparation of 3-methyl-2-cyclohexenone **3** starting from ethyl acetoacetate **1** and butenone **2** was chosen as the model reaction under microwave activation.

The exploration of the best reaction conditions was investigated by studying the influence of 11 variables: the type of ecocatalyst® and its catalytic loading and hence its composition in Ca, K, Mg and Na, the Thermal Treatment (TT) of the ecocatalyst®, the quantity of glycerol, the reaction time and the reaction temperature. Each of these variables were optimised following a one-variable-at-a-time (OVAT) strategy (see all tested conditions with the corresponding yields in Table S2). The variables and the corresponding yields of 38 reactions were statistically analysed by calculating the Spearman correlation matrix and associated p-values (Fig. 2(a)). The Spearman correlations of the 11 variables with the reaction yield were represented as circles whose surface is proportional to the intensity of the correlation and whose ordinate corresponds to the relative correlation.

The reaction conditions and the composition, hence the type, of ecocatalyst® displayed the most important correlations with the yield. Indeed, the quantity of Mg (0 – 0.11 equiv.) and the reaction temperature (100 – 220 °C), respectively showed high and positive correlations (0.61 and 0.60), which were also statistically significant (p-value of 0.001 and 0.002). The reaction time showed a medium and positive correlation with the yield. One variable, which is the only one to present a negative but still medium correlation with the yield, was the absence

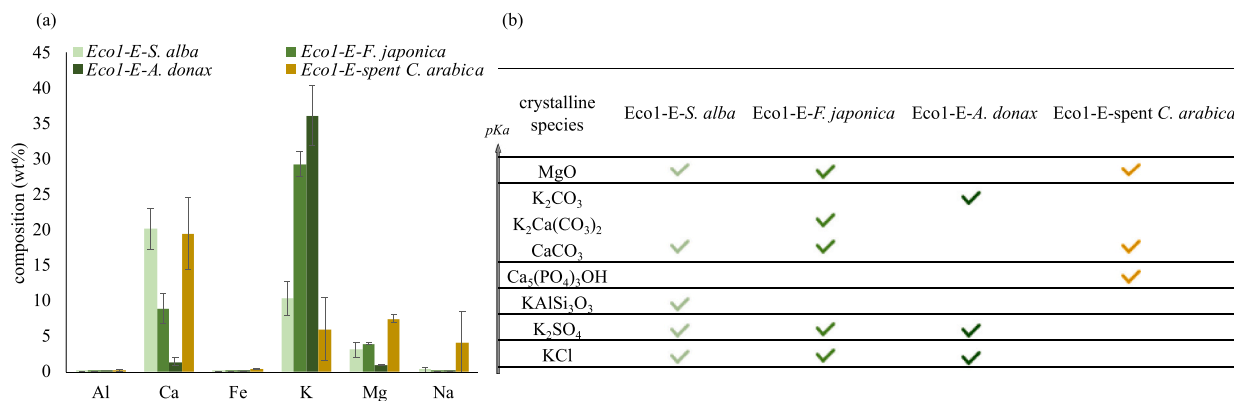


Fig. 1. (a) Elemental composition of ecocatalysts® determined by MP-AES. MP-AES data are the mean \pm SD of three independent preparations of ecocatalysts®. (b) Crystalline species of ecocatalysts® detected by XRPD analysis.

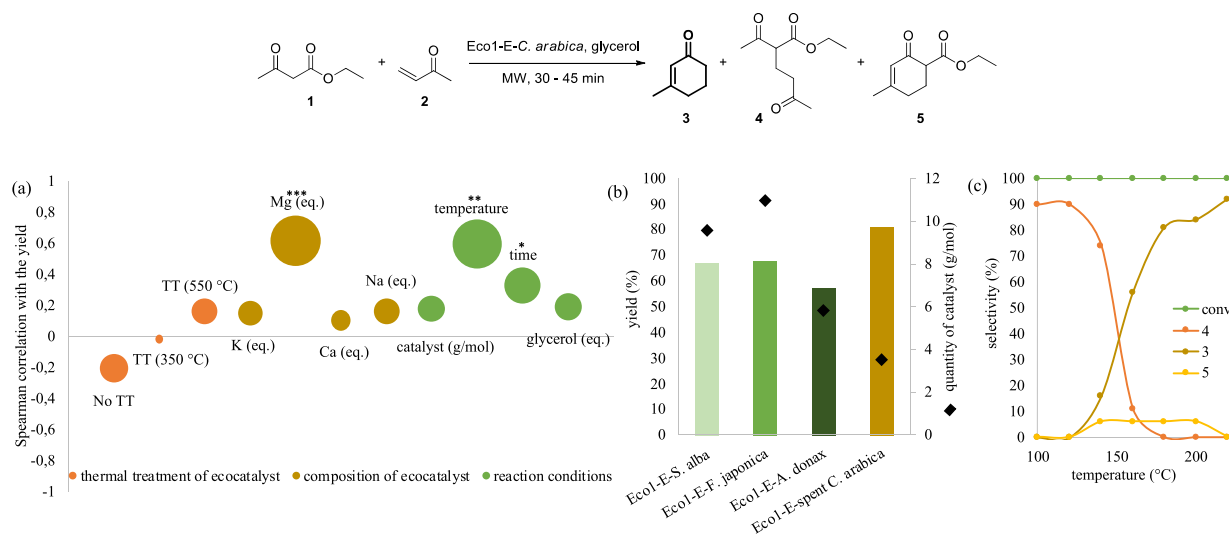


Fig. 2. Optimisation of the model reaction conditions of ethyl acetoacetate **1** and butenone **2** under microwave activation. (a) Spearman correlations of 11 variables with the yield (0 – 92%) from the model reaction carried out on 38 experiments. Spearman correlations are represented as circles whose surface is proportional to the absolute value and the ordinate is the relative value. *** p-value < 0.001, ** p-value < 0.01 and * p-value < 0.05. Range of variables studied: thermal treatment of ecocatalysts® (none, 350 °C and 550 °C), composition of ecocatalyst® (equivalent of Ca (0 – 0.16 equiv.), K (0 – 0.21 equiv.), and Na (0 – 0.03 equiv.), Mg (0 – 0.11 equiv.)), and reaction conditions (quantity of glycerol (0 – 0.5 equiv.), reaction time (30 – 90 min), reaction temperature (100 – 220 °C)); (b) Comparison of ecocatalysts® (*Eco1-E-S. alba*, *Eco1-E-F. japonica*, *Eco1-E-A. donax* and *Eco1-E-spent C. arabica*) efficiency in the model reaction with the optimised conditions (180 °C (MW), 30 min, glycerol (0.5 equiv.), ecocatalyst® (0.01 equiv. of Mg, 0.02 equiv. of Ca or 0.05 equiv. of K)); (c) Influence of the reaction temperature over the formation of side products in the model reaction (100 – 220 °C (MW), 30 min, glycerol (0.5 equiv.), *Eco1-E-spent C. arabica* (0.01 equiv. of Mg, 0.02 equiv. of Ca)). Yields were quantified by GC-FID analysis.

of TT of the ecocatalyst®.

Bearing in mind that the quantity of Mg within the ecocatalyst®, its preparation and the reaction temperature were key parameters for the reaction, the four ecocatalysts®, prepared at 550 °C and introduced in the same molar equivalent of Mg, were compared at 180 °C during 30 min (Fig. 2(b)). *Eco1-E-spent C. arabica* was the most efficient as it led to the highest yield with the lowest quantity of catalyst (81% as the average yield of 9 experiments).

Furthermore, the reaction temperature playing an important role on the yield, the reaction was studied using the best ecocatalyst®, *Eco1-E-spent C. arabica*, at higher temperatures (Fig. 2(c)). The highest temperature of 220 °C led to the best conversion and selectivity towards **3** (100 and 92%). Indeed, the side products **4** and **5**, which were observed at lower temperature, were transformed at 220 °C into the desired cyclohexenone **3**.

3.2.2. Environmental impact assessment through green metrics comparison

The reaction conditions as well as the associated workup procedure


were compared to similar strategy processes from literature. To do so, several green metrics were calculated – the E-factor evaluating the production of wastes, the process mass intensity (PMI) which has been detailed for the workup procedure and allows to depict the E-factor in details, the energy consumption during the reaction and the space-time-yield (STY) representing the time and reactor volume required for 1 g of product, the turn over number (TON) representing the lifetime robustness of a catalyst and the turn over frequency (TOF) measuring the TON per unit time – and the presence of hazardous compounds was flagged (Table 1). The methods of calculation are described in the ESI.

Usually, strong and synthetic Brønsted bases, such as alcoholates, are used to promote the annulation reaction for a few hours at reflux followed by a decarboxylation step, which requires higher or longer heating, leading to moderate and good yields (55 and 76%) [15–17]. A different approach was studied in neutral conditions using hexamethylphosphoramide in the presence of lithium chloride and led to a similar yield of 73% [31,32].

Both approaches presented good yields and some good metrics in

Table 1

Comparison of green metrics. Red flag indicates hazardous compounds (HMPA) according to the CLP classification. *Isolated yields. [‡]Crude yield. [#]Recycling of the ecocatalyst® was conducted at a larger scale (x 4) on 12 reactors in parallel in similar conditions. TON and TOF were calculated from the yields of each run given in Table S4. ND: not determined as the product was not isolated from the crude reaction mixture.

ref	catalyst (origin)	method	conditions	yield	E-factor	PMI (PMI workup)	energy (°C.h)	STY (g.h ⁻¹ .L ⁻¹)	TONTOF (h ⁻¹)
[15]	<i>t</i> -BuOK (synthetic)	batch	20 h, 83 °C	76%*	307	310 (298)	1173	46	ND
[16,17]	NaOMe (synthetic)	batch	5 h, 81 °C then 1 h, 100 °C	55%*	29	33 (20)	355	12	ND
[31,32]	LiCl, HMPA 	batch	2 h, 160 °C	73% [‡]	ND	ND	270	ND	ND
present work	Eco1-E-spent <i>C. arabica</i> (biosourced)	batch	20 h, 180 °C	68%*	7	9	3100	2	ND
		microwave	45 min, 220 °C	90%*	5	(4)	162	49	1718 [#]
						7 (3)			572 [#]

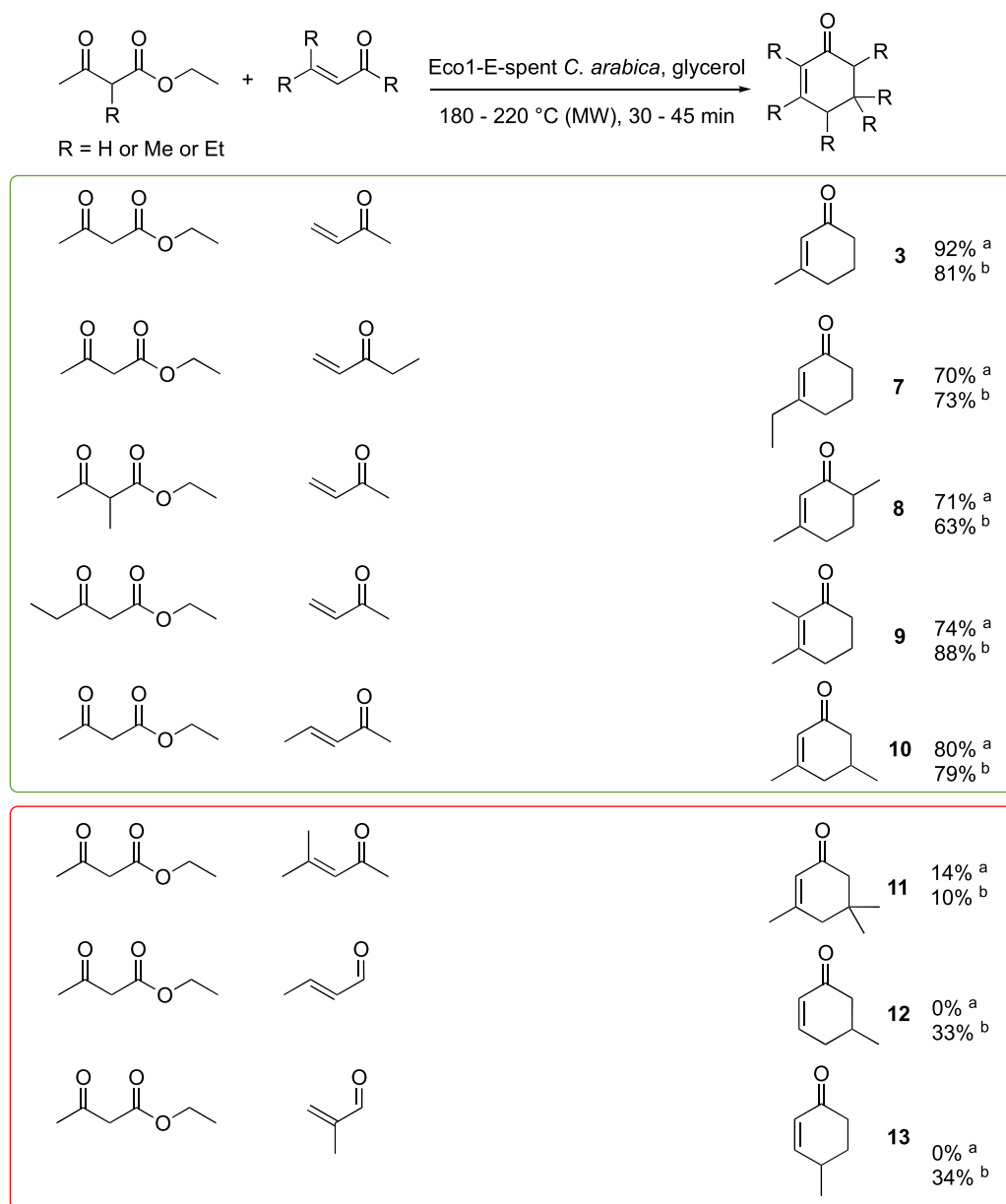


Fig. 3. Exploration of substrate scope (β-keto ester (2 equiv.), Eco1-E-spent *C. arabica* (0.01 equiv. of Mg and 0.02 equiv. of Ca), α,β-unsaturated ketone (or ketal) (1 equiv.) and glycerol (0.5 equiv.), ^a 220 °C, 45 min; ^b 180 °C, 30 min). Yields were quantified by GC-FID analysis for the model reaction or by ¹H NMR using mesitylene as internal standard for the other reactions.

individual categories but the present work based on ecocatalysis led to the best yield (90%) and the best green metrics in every category when the reaction was conducted under microwave activation. In details, the microwave activation led to a significant decrease of the reaction time, which is related to a low energy consumption and a high STY compared to the other reactions conducted in batch. The E-factor, which evaluates the wastes generated during the reaction and workup procedure, is much lower compared to other processes. Taken together, the PMI and PMI workup show that the low value of E-factor is due to combined efforts to perform the reaction solvent-free, with a minimum of reagent in excess and to perform the work up using a minimum of organic and aqueous layers.

Moreover, the ecocatalyst® was the first catalyst that could be recycled and reused for the preparation of cyclohexenones. Recycling study of Eco1-E-spent *C. arabica* was performed on a larger scale, also illustrating the scale-up of the reaction. Eco1-E-spent *C. arabica* could be reused up to 3 runs with a loss of activity of less than 9%, the 4th and 5th runs leading to lower yields (Table S4). The TON and TOF were quite high thanks to the low catalytic loading and a short time reaction needed to obtain a high yield.

Finally, the presented work also stands out by the use of non-hazardous ecocatalysts® related to their natural origin. Indeed, in addition of being biosourced, Eco1-E-spent *C. arabica* was derived from a waste that was upcycled by a direct and simple preparation by thermal treatment, leading to a good but perfectible Life Cycle Analysis (LCA). Indeed, the thermal treatment leads to a weight loss of 97–99% according to the biomass. In order to improve the LCA, the combustion heat could be used in heating systems, as it had been suggested for agromining, and the produced gases could be captured in chemical trap.

3.3. Scope of the tandem reaction for the synthesis of substituted cyclohexenones 3–13

The best ecocatalyst®, Eco1-E-spent *C. arabica*, was used to extend the synthesis to other methyl and ethyl substituted cyclohexenones (Fig. 3).

The strategy has been successfully applied to the synthesis of mono- and disubstituted cyclohexenones 7–10 as 3-ethyl, 3,6-dimethyl, 2,3-dimethyl and 3,5-dimethyl cyclohexenones with good yields (70 – 88%). However, the use of α,β -unsaturated aldehydes instead of α,β -unsaturated ketones did not conduct to the cyclohexenones 11–13 in satisfying yields. Indeed, methacrolein and crotonaldehyde led to their non-surprisingly polymerisation, which has been previously described in basic conditions [33–38]. Furthermore, the use of 4-methyl-3-penten-2-one led to a poor conversion of 17%, probably due to steric hindrance.

In general, the increase of temperature has not led to a significant increase in yield, which is interesting for regulating the energy consumption.

4. Discussion

4.1. Investigation of the active species within ecocatalysts®

Before investigating the nature of the active species of the best ecocatalyst®, Eco1-E-spent *C. arabica*, the reproducibility for the synthesis of 3-methyl-2-cyclohexenone catalysed by Eco1-E-spent *C. arabica* was studied over time. Three ecocatalysts of Eco1-E-spent *C. arabica* were prepared coming from different batches of coffee grounds, collected in three periods of time (winter, summer and autumn). Their elemental composition varies in K and Na, but varies little in Mg (Fig. 1(a)). The three Eco1-E-spent *C. arabica* were hence introduced in the same molar equivalent of Mg, since it has been determined as a key parameter of the reaction. The three ecocatalysts® led to similar yields independently of the batch of biomass (Fig S5), illustrating the reproducibility of the method.

4.1.1. Comparison of reactivities of Eco1-E-spent *C. arabica* and commercial salts

The high efficiency of Eco1-E-spent *C. arabica* was investigated by studying the individual reactivity of commercial salts that were found in its crystalline structure: MgO, CaCO₃ and Ca₅(PO₄)₃OH (Fig. 4(a)). Magnesium oxide introduced in the same molar quantities of Mg as in Eco1-E-spent *C. arabica* led to the highest yield of 71% and the closest to the yield obtained with Eco1-E-spent *C. arabica* (81% as the average yield of 7 experiments). The calcium salts, calcium carbonate or hydroxyapatite, led to low yields of 14 and 13%. A mixture of the three salts led to a similar yield as the one obtained with only MgO.

Suspecting that the active species in Eco1-E-spent *C. arabica* could be MgO, ecocatalysts® which have been prepared at different temperatures were engaged in the model reaction: another ecocatalyst® derived from spent coffee ground prepared at a lower temperature of 350 °C and a non-thermally treated spent coffee ground. Commercial MgO used in chemical catalysis is usually prepared at 700 – 1000 °C [39,40]. But the apparition of MgO from magnesite (MgCO₃) can occur at lower temperature between 400 and 750 °C [41,42]. In any cases, both Eco1-E-spent *C. arabica* (350 °C) and spent coffee ground should not contain any MgO. As expected, the reactivity of these last two collapsed. Moreover, the quantity of catalyst was much higher, due to the lower ratio of Mg and the remaining organic matter, and such high quantity of ecocatalyst® disrupted the reaction stirring, also contributing to the lower yields.

The activity of MgO and Eco1-E-spent *C. arabica* was compared at different concentrations of Mg in the reaction mixture (Fig. 4(b)). Their activity gave similar profiles, supporting that the active species within Eco1-E-spent *C. arabica* was MgO.

4.1.2. Extensive morphological and structural characterisation of Eco1-E-spent *C. arabica*

The morphology of Eco1-E-spent *C. arabica* was determined via scanning electron microscopy (SEM) and nitrogen sorption experiments (Fig. 5). In general, ecocatalysts® or biomass derived from a unique thermal treatment are powder-like materials with low porosity [39,43]. In the present case, the nitrogen sorption isotherm of Eco1-E-spent *C. arabica* indicates a specific surface area S_{BET} of 10 m²/g. The nitrogen uptake takes place essentially at high relative pressures ($p/p^0 > 0.9$), pointing towards interparticular porosity, i.e., porosity that is formed at the interstitial space between the particles. SEM microscopy confirms this assumption as the SEM image of Eco1-E-spent *C. arabica* essentially shows two populations of particles: agglomerated spherical nanoparticles of a diameter in the range of 50–200 nm and larger micrometric size particles. Nitrogen sorption and SEM analyses therefore give concordant results regarding the morphology of the material.

Despite its low porosity, the Eco1-E-spent *C. arabica* displays high catalytic activity, that cannot be explained by the low specific surface area.

The similar reactivity of Eco1-E-spent *C. arabica* and MgO strongly suggested that MgO might be the active species within the ecocatalyst®, however further characterisation was needed to conclude that all the Mg species corresponded to MgO. XRPD analyses attested the presence of MgO and no other crystalline adducts but considering that this technique only shows the crystalline species within a powder, ²⁵Mg solid-state MAS NMR experiments were conducted on Eco1-E-spent *C. arabica* and on commercial MgO to remove any doubt (Fig. 6(a)). Both catalysts were introduced with the same dilute of Mg (8.1% in average, see Fig. 1(a)) but do not present the same density, the MAS NMR spectra were normalised to respect the quantity of powder introduced in the rotor. Both MAS spectra display an identical peak centred on 25.8 ppm for commercial MgO and 26 ppm for Eco1-E-spent *C. arabica*; such chemical shifts are consistent with MAS spectra of MgO from literature [44]. No other peak was detected on the spectrum of Eco1-E-spent *C. arabica* supporting that one Mg species was mainly present as MgO in the ecocatalyst®.

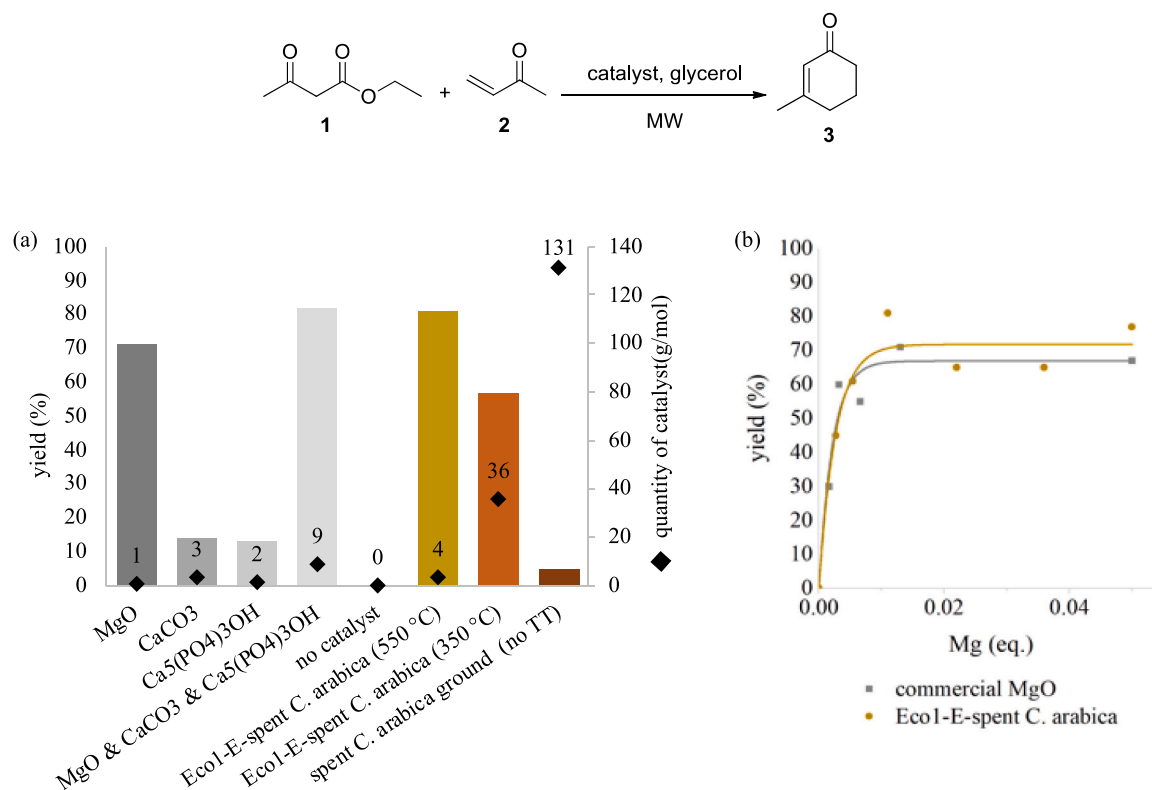


Fig. 4. Evaluation of the active species within Eco1-E-spent *C. arabica* in the model reaction. (a) Comparison of the catalytic efficiency of commercial salts and Eco1-E-spent *C. arabica* (ethylacetoacetate (2 equiv.), Eco1-E-spent *C. arabica* (0.01 equiv. of Mg and 0.016 equiv. of Ca), 3-buten-2-one (1 equiv.) and glycerol (0.5 equiv.), 180 °C (MW), 30 min). Yields were quantified by GC-FID analysis. The molar quantities of Mg and Ca, that were introduced in the reaction mixture as commercial salts, were identical to the one present in Eco1-E-spent *C. arabica*. (b) Evolution of the yield versus the equivalence of Mg in MgO and in Eco1-E-spent *C. arabica* introduced in the reaction.

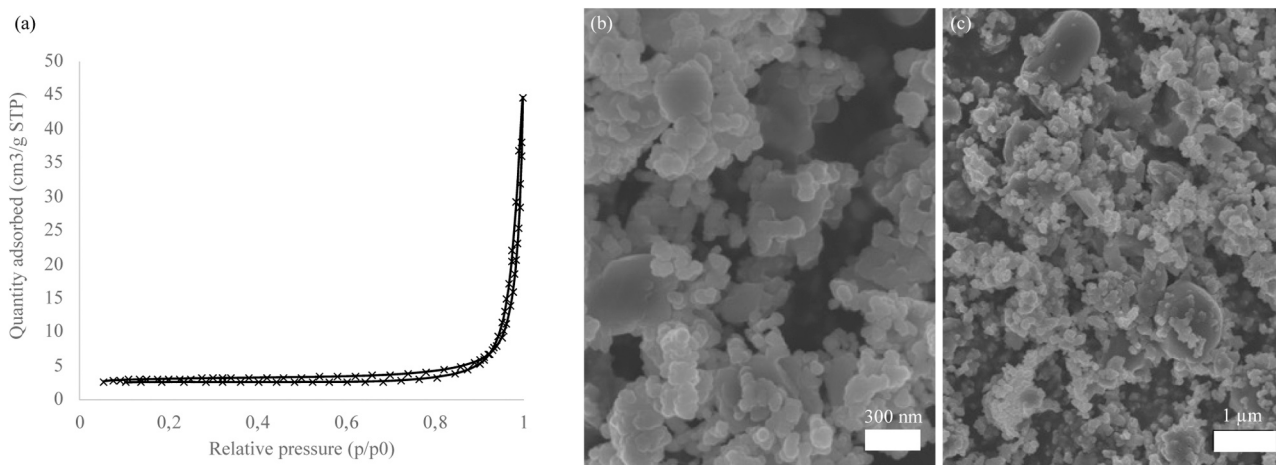


Fig. 5. Morphology of Eco1-E-spent *C. arabica*. (a) Nitrogen sorption experiments; (b) Representative example of SEM image.

To support solid-state MAS NMR spectroscopy of ²⁵Mg observations, XPS analyses were performed on Eco1-E-spent *C. arabica* and on commercial MgO (Fig. 6(b-d)). The XPS spectrum of Eco1-E-spent *C. arabica* was more complex than commercial MgO due to the presence of other species related to its plant origin. However, the binding energy (BE) of Mg2p and Mg2s of Eco1-E-spent *C. arabica* was identical to the ones of commercial MgO (Fig. 6(b)). Deconvolution of the fitted envelopes shows the presence of three species of magnesium in both catalysts (commercial MgO and ecocatalyst®): MgO (70 and 79%), Mg(OH)₂ (18 and 14%) and Mg(CO₃)₂ (12 and 6%). The presence of other Mg species

than MgO in both catalysts are not surprising since XPS analyses only showed the surface sample and is not entirely representative of the bulk. Anyway, both catalysts present quasi-identical XPS spectra, supporting that the Mg species within Eco1-E-spent *C. arabica* corresponds to MgO.

4.2. Investigation of the reaction mechanism catalysed by MgO and DFT calculations

Considering the unexpected and high reactivity of Eco1-E-spent *C. arabica* and MgO in the synthesis of cyclohexenones, the reaction

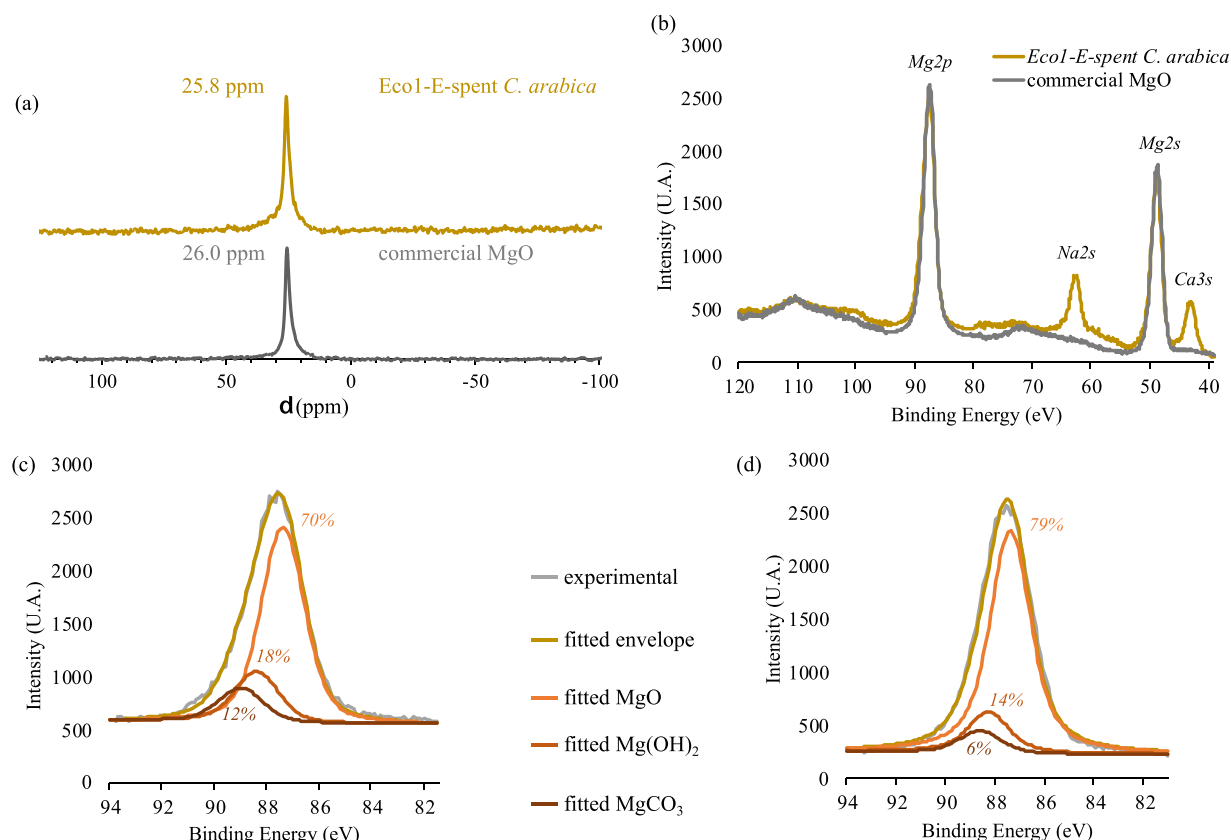


Fig. 6. Characterisation of Eco1-E-spent *C. arabica* and comparison to commercial MgO. (a) ^{25}Mg solid-state MAS NMR spectra of Eco1-E-spent *C. arabica* and commercial MgO dilute at 8.1% with a spectral window of 120: –100 ppm. (b) Superimposition of XPS spectra of Eco1-E-spent *C. arabica* and MgO with a spectral window of +40: +120 eV. (c) XPS spectrum and fitted curves of Mg2p of Eco1-E-spent *C. arabica*. (d) XPS spectrum and fitted curves of Mg2p of commercial MgO.

mechanism was discussed using the relative Gibbs energy of intermediate compounds calculated by DFT using the B3LYP-GD3BJ/def2svp level of computation as implemented in the Gaussian 16 program [45] (Fig. 7).

The preparation of cyclohexenones is not straightforward starting from butenone **2** and ethylacetoacetate **1**, as in basic conditions they can lead to two synthetic routes: the desired tandem annulation-decarboxylation (Fig. 7 in green) or the tandem annulation-crotonisation (Fig. 7 in red). Intermediates of both routes were simulated by DFT and their relative Gibbs energy was compared in the presence of the active species within the best ecocatalyst®, MgO. MgO was represented as a stable cluster of $(\text{MgO})_{10}$ to mimic the surface of magnesia while optimising the calculation time. The Michael addition of ethylacetoacetate **1** onto butanone **2** was catalysed by the expected Brønsted basicity but also the Lewis acidity of MgO. Indeed, interactions between the carbonyls of ethylacetoacetate **1** and Mg of $(\text{MgO})_{10}$ ($d_{\text{C=O} \cdots \text{Mg}} = 2.10 \text{ \AA}$) were spontaneously observed and converged to a lower energy complex ($\Delta E = -18 \text{ kcal.mol}^{-1}$), illustrating the Lewis acidity of MgO. As the Michael addition of ethylacetoacetate **1** onto butanone **2** started by the deprotonation of ethylacetoacetate **1**, the acidic proton was added onto the closest oxygen of $(\text{MgO})_{10}$; the generated $[\text{enolate } 1' \cdots (\text{MgO})_{10}\text{H}]$ complex converged to a lower energy ($\Delta E = -19 \text{ kcal.mol}^{-1}$), illustrating the Brønsted basicity of MgO. This Michael addition was observed experimentally as the Michael adduct **4** was mostly observed at 100 – 150 °C (Fig. 2(c)).

Then intramolecular aldol condensation of **4'** was also favoured by the basic properties of MgO leading to the key tertiary alcoholate **14'**. This alcoholate **14'** could now follow two possible modes of reaction sequences. However, the presence of MgO stabilises the alcoholate **14'** avoiding its protonation ($\Delta E = -30 \text{ kcal.mol}^{-1}$) and activates the ester moiety ($d_{\text{C=O} \cdots \text{Mg}} = 2.20 \text{ \AA}$), leading to an intramolecular lactonisation

and giving the bicyclic lactone **15**. Indeed, the product **16** resulting from the protonation of the alcoholate requires more energy than the lactonisation. At last, MgO favours the lactonisation followed by a spontaneous decarboxylation instead of the protonation followed by the crotonisation, as only 6% of the β -ketoester **5** was observed at 150 – 200 °C (Fig. 2(c)). Such theoretical analysis was consistent with the experimental results as only the decarboxylation product, the desired cyclohexenone **3**, was observed at 220 °C (Fig. 2(c)).

5. Conclusion

The synthesis of substituted cyclohexenones was revisited thanks to ecocatalysis while respecting the principles of green chemistry. Ecocatalysts® derived from biomass wastes efficiently catalysed the reaction with better yields than previously reported. One ecocatalyst® derived from spent coffee ground was particularly efficient (92% in only 30 min) and could be recycled and reused up to 3 runs without any significant loss of activity. The whole process was assessed by calculating 7 green metrics, among which were found an excellent E-factor, a low energy consumption, a correct STY and high TON and TOF. The catalytically active species in the ecocatalyst® derived from spent coffee ground could be clearly identified as MgO through synthetic experiments and characterisation by XRPD, solid-state NMR and XPS. The activity of MgO was also supported by DFT calculations allowing to revisit the reaction mechanism.

However, one might wonder the advantage of using ecocatalysis instead of conventional MgO. Conventional MgO is produced for a catalytic use by heating at high temperature (700 °C - 1000 °C) MgCO_3 obtained by mining extractions [39,40], mainly opencast, or MgCl_2 obtained from seawater and salt deposits treated by CaO [46], which itself requires another preparation. The ecocatalysts® allows the

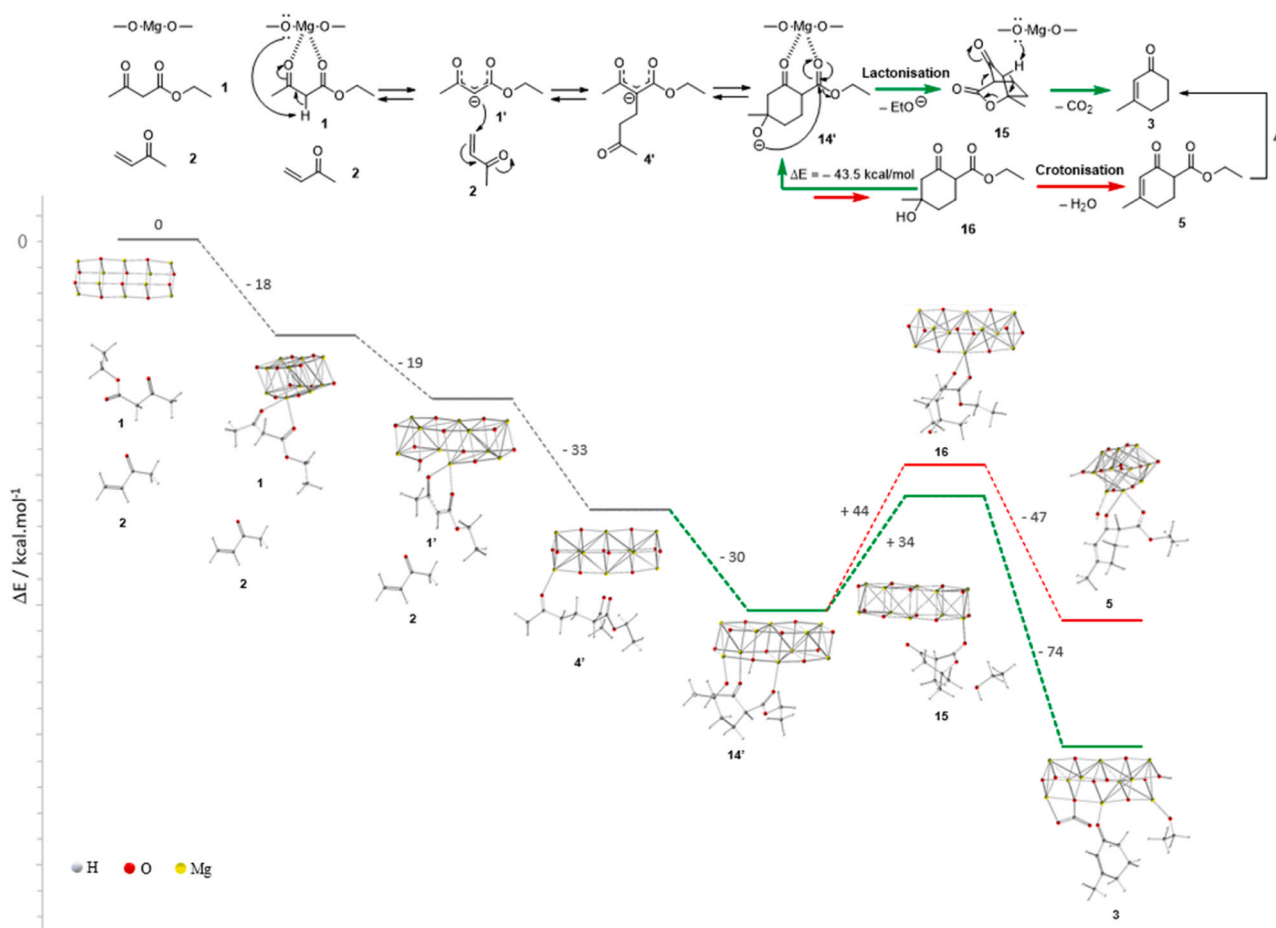


Fig. 7. Role of MgO in the reaction mechanism supported by Gibbs energy of intermediate compounds calculated by DFT.

valorisation of an abundant biomass waste, which is easily transformed at a moderate temperature of 550 °C. The ecocatalysts® give access to a new generation of biosourced MgO with similar reactivity and exhibits environmental benefits in comparison to conventional MgO.

CRediT authorship contribution statement

Franck pelissier: Validation, Formal analysis, Data curation. **Laure Liénart:** Writing – review & editing, Investigation, Formal analysis, Data curation. **Yves-Marie Legrand:** Writing – review & editing, Visualization, Validation, Investigation, Data curation. **Eddy Petit:** Validation, Investigation, Formal analysis. **Claude Grison:** Writing – review & editing, Validation, Supervision, Methodology, Funding acquisition, Formal analysis, Data curation, Conceptualization. **Philippe Gaveau:** Validation, Investigation, Data curation. **Peter Hesemann:** Validation, Investigation, Data curation. **Claire Marie Grison:** Writing – review & editing, Writing – original draft, Validation, Supervision, Methodology, Investigation, Formal analysis, Conceptualization.

Declaration of Competing Interest

The authors declare that they have no known competing financial interests or personal relationships that could have appeared to influence the work reported in this paper.

Data availability

Data will be made available on request.

Acknowledgements

The authors would like to thank BIOINSPIR for harvesting *Fallopia japonica*, Bruno Breton and Adrien Messean from Conservatoire d'espaces naturels des Hauts de France for harvesting *Salix alba*. The authors would like to thank Bertrand Rebière, Arie Van der Lee and Bernard Fraisse for performing SEM and XRPD analyses. The authors would also like to thank Danielle Laurencin for her help with the MAS NMR experiments. This work was granted access to the HPC resources of IDRIS under the allocation 2023-AD010813663R1 made by GENCI. Finally, the authors gratefully acknowledge financial support from the regional funds (Occitanie, Graine 2021 - Resilience project).

Appendix A. Supporting information

Supplementary data associated with this article can be found in the online version at doi:10.1016/j.apcatb.2024.123888.

References

- [1] X. Yang, J. Wang, P. Li, Recent progress on asymmetric organocatalytic construction of chiral cyclohexenone skeletons, *Org. Biomol. Chem.* 12 (2014) 2499–2513, <https://doi.org/10.1039/C3OB42293C>.
- [2] A.J.D. Silvestre, M. Válega, J.A.S. Cavaleiro, Chemical transformation of 1,8-cineole: synthesis of seudone, an insect pheromone, *Ind. Crops Prod.* 12 (2000) 53–56, [https://doi.org/10.1016/S0926-6690\(99\)00067-9](https://doi.org/10.1016/S0926-6690(99)00067-9).
- [3] S.Y. Shin, J. Park, Y. Jung, Y.H. Lee, D. Koh, Y. Yoon, Y. Lim, Anticancer activities of cyclohexenone derivatives, *Appl. Biol. Chem.* 63 (2020) 82, <https://doi.org/10.1186/s13765-020-00567-1>.
- [4] High Pressure Diels–Alder Reaction, in: *Diels–Alder React.*, John Wiley & Sons, Ltd, 2001, pp. 205–249, <https://doi.org/10.1002/0470845813.ch5>.
- [5] B.L. Feringa, R. Naasz, R. Imbos, L.A. Arnold, Copper-catalyzed Enantioselective Conjugate Addition Reactions of Organozinc Reagents. *Mod. Organocopper Chem.*,

- John Wiley & Sons, Ltd, 2002, pp. 224–258, <https://doi.org/10.1002/3527600086.ch7>.
- [6] Y. Sohtome, A. Tanatani, Y. Hashimoto, K. Nagasawa, Development of bis-thiourea-type organocatalyst for asymmetric Baylis–Hillman reaction, *Tetrahedron Lett.* 45 (2004) 5589–5592, <https://doi.org/10.1016/j.tetlet.2004.05.137>.
 - [7] E. Toromanoff, Steric Course of the Kinetic 1,2 Addition of Anions to Conjugated Cyclohexenones. *Top. Stereochem.*, John Wiley & Sons, Ltd, 1967, pp. 157–198, <https://doi.org/10.1002/9780470147115.ch3>.
 - [8] D. Jyothi, S. HariPrasad, Cyclic α -Alkylvinyl Anionic Synthons: A Novel Synthesis of 2-Trimethylsilyl-3-methyl-cyclohexenone by the Wurtz–Fittig Coupling Reaction, *Synth. Commun.* 39 (2009) 875–879, <https://doi.org/10.1080/00397910802432196>.
 - [9] K. Shaw, S. Niyogi, V. Bisai, Catalytic enantioselective total synthesis of (–)-ar-Tenuifolene, *Tetrahedron Lett.* 61 (2020) 151850, <https://doi.org/10.1016/j.tetlet.2020.151850>.
 - [10] L.-Q. Li, M.-M. Li, D. Chen, H.-M. Liu, H. Geng, J. Lin, H.-B. Qin, Catalytic asymmetric formal total synthesis of (+)-dichroanone and (+)-taiwaniaquinone H, *Tetrahedron Lett.* 55 (2014) 5960–5962, <https://doi.org/10.1016/j.tetlet.2014.08.110>.
 - [11] A.J. Birch, 119. Reduction by dissolving metals. Part III, *J. Chem. Soc. Resume* (1946) 593, <https://doi.org/10.1039/jr9460000593>.
 - [12] A.E. Goetz, J. Arcari, S.W. Bagley, R. Hicklin, L. Jin, Z. Jin, X. Li, Z. Liu, J. C. McWilliams, M.D. Parikh, T. Potter, W.J. Smith, L. Sun, J. Trujillo, P. Wang, X. Zhao, Demonstration of a multikilogram-scale birch reduction and evaluation of alternative synthetic routes to a ketalized cyclohexene derivative, *Org. Process Res. Dev.* (2023), <https://doi.org/10.1021/acs.oprd.3c00141>.
 - [13] H.J. Bestmann, R. Pichl, R. Zimmermann, Phosphanalkylene, 53. Synthese von α,β 1-ungesättigten Cycloalkanonen aus Bis[(1-acylalkyliden)1-triphenylphosphoranen] – Eine Methode zur Überführung von Carbonsäure-Anhydriden in carbocyclische und heterocyclische Verbindungen, *Chem. Ber.* 126 (1993) 725–731, <https://doi.org/10.1002/cber.19931260324>.
 - [14] M. Bezanson, J. Pottel, R. Bilbeisi, S. Toumieux, M. Cueto, N. Moitessier, Stereo- and regioselective synthesis of polysubstituted chiral 1,4-oxazepanes, *J. Org. Chem.* 78 (2013) 872–885, <https://doi.org/10.1021/jo3021715>.
 - [15] J. Danino, Carbene rearrangements: intramolecular interaction of a triple bond with a carbene center, *Org. State University*, 1982.
 - [16] B.-D. Chong, Y.-I. Ji, S.-S. Oh, J.-D. Yang, W. Baik, S. Koo, Highly efficient synthesis of methyl-substituted conjugate cyclohexenones, *J. Org. Chem.* 62 (1997) 9323–9325, <https://doi.org/10.1021/jo970145x>.
 - [17] K.-D. Umland, A. Palisse, T.T. Haug, S.F. Kirsch, Domino reactions consisting of heterocyclization and 1,2-migration-redox-neutral and oxidative transition-metal catalysis, *Angew. Chem. Int. Ed.* 50 (2011) 9965–9968, <https://doi.org/10.1002/anie.201103961>.
 - [18] C. Grison, Y. Lock Toy Ki, Ecocatalysis, a new vision of green and sustainable chemistry, *Curr. Opin. Green. Sustain. Chem.* 29 (2021) 100461, <https://doi.org/10.1016/j.cogsc.2021.100461>.
 - [19] C. Bihanic, K. Richards, T.K. Olszewski, C. Grison, Eco-Mn ecocatalysts: toolbox for sustainable and green lewis acid catalysis and oxidation reactions, *ChemCatChem* 12 (2020) 1529–1545, <https://doi.org/10.1002/cctc.201901845>.
 - [20] P.-A. Deyris, P. Adler, E. Petit, Y.-M. Legrand, C. Grison, Woody species: a new bio-based material for dual Ca/Mg catalysis with remarkable Lewis acidity properties, *Green. Chem.* 21 (2019) 3133–3142, <https://doi.org/10.1039/C9GC00770A>.
 - [21] P.-A. Deyris, C. Grison, Nature, ecology and chemistry: An unusual combination for a new green catalysis, *Ecocatalysis*, *Curr. Opin. Green. Sustain. Chem.* 10 (2018) 6–10, <https://doi.org/10.1016/j.cogsc.2018.02.002>.
 - [22] V. Escande, C. Poullain, G. Clavé, E. Petit, N. Masquelez, P. Hesemann, C. Grison, Bio-based and environmental input for transfer hydrogenation using EcoNi(0) catalyst in isopropanol, *Appl. Catal. B Environ.* 210 (2017) 495–503, <https://doi.org/10.1016/j.apcatb.2017.04.023>.
 - [23] G. Clavé, F. Pelissier, S. Campidelli, C. Grison, Ecocatalyzed Suzuki cross coupling of heteroaryl compounds, *Green. Chem.* 19 (2017) 4093–4103, <https://doi.org/10.1039/C7GC01672G>.
 - [24] V. Escande, L. Garoux, C. Grison, Y. Thillier, F. Debart, J.-J. Vasseur, C. Boulanger, C. Grison, Ecological catalysis and phytoextraction: symbiosis for future, *Appl. Catal. B Environ.* 146 (2014) 279–288.
 - [25] H.E. Roy, A. Pauchard, P. Stoett, T. Renard Truong, S. Bacher, B.S. Galil, P. E. Hulme, T. Ikeda, K.V. Sankaran, M.A. McGeoch, L.A. Meyerson, M.A. Nuñez, A. Ordóñez, S.J. Rahlao, E. Schwindt, H. Seebens, A.W. Sheppard, V. Vandvik, IPBES invasive alien species assessment: summary for policymakers, *Zenodo* (2023), <https://doi.org/10.5281/zenodo.8314303>.
 - [26] C. Grison, V. Escande, J. Biton, *Ecocatalysis* - 1st Edition, 1st Edition, 2015. (<https://shop.elsevier.com/books/ecocatalysis/grison/9781-78548-030-0>) (accessed November 23, 2023).
 - [27] Y. Lock Toy Ki, A. Garcia, F. Pelissier, T.K. Olszewski, A. Babst-Kostecka, Y.-M. Legrand, C. Grison, Mechanochemistry and eco-bases for sustainable michael addition reactions, *Molecules* 27 (2022) 3306, <https://doi.org/10.3390/molecules27103306>.
 - [28] C. Adamo, G.E. Scuseria, V. Barone, Accurate excitation energies from time-dependent density functional theory: assessing the PBE0 model, *J. Chem. Phys.* 111 (1999) 2889–2899, <https://doi.org/10.1063/1.479571>.
 - [29] F. Weigend, R. Ahlrichs, Balanced basis sets of split valence, triple zeta valence and quadruple zeta valence quality for H to Rn: design and assessment of accuracy, *Phys. Chem. Chem. Phys.* 7 (2005) 3297–3305, <https://doi.org/10.1039/B508541A>.
 - [30] S. Grimme, S. Ehrlich, L. Goerigk, Effect of the damping function in dispersion corrected density functional theory, *J. Comput. Chem.* 32 (2011) 1456–1465, <https://doi.org/10.1002/jcc.21759>.
 - [31] Y. Ozaki, A. Kubo, S.-W. Kim, A method for the cyclic enone synthesis using lithium chloride – hexamethylphosphoramide system, *Chem. Lett.* 22 (1993) 993–994, <https://doi.org/10.1246/cl.1993.993>.
 - [32] Y. Ozaki, A. Kubo, K. Okamura, S.-W. Kim, A new method for the preparation of michael adducts and cyclic enones using lithium chloride-hexamethylphosphoramide system, *Chem. Pharm. Bull. (Tokyo)*. 43 (1995) 734–737, <https://doi.org/10.1248/cpb.43.734>.
 - [33] J.N. Koral, Crotonaldehyde polymerization, *J. Polym. Sci.* 61 (1962), <https://doi.org/10.1002/pol.1962.1206117218>.
 - [34] H. Rubinstein, Intermediates in the synthesis of Xanthophyll and Zeaxanthin, *J. Org. Chem.* 27 (1962) 3886–3887, <https://doi.org/10.1021/jo01058a031>.
 - [35] Ed.F. Degering, T. Stoudt, Polymerization of acetaldehyde and crotonaldehyde catalyzed by aliphatic tertiary amines, *J. Polym. Sci.* 7 (1951) 653–656, <https://doi.org/10.1002/pol.1951.120070609>.
 - [36] I.V. Andreeva, M.M. Koton, Yu.P. Getmanchuk, L.Ya Madorsikaya, E.I. Pokrovskii, A.I. Koltsov, Polymerization of α -methacrolein and the structure of the polymers, *J. Polym. Sci. Part C. Polym. Symp.* 16 (1967) 1409–1421, <https://doi.org/10.1002/polc.5070160319>.
 - [37] J.N. Koral, The anionic polymerization of crotonaldehyde, *Makromol. Chem.* 62 (1963) 148–163, <https://doi.org/10.1002/macp.1963.020620117>.
 - [38] M.M. Koton, I.V. Andreyeva, Yu.P. Getmanchuk, L.Ya Madorsikaya, Ye. I. Koltsov, Polymerization of α -methacrolein and the structure of the polymers prepared by anionic polymerization, *Polym. Sci. USSR* 7 (1965) 2232–2241, [https://doi.org/10.1016/0032-3950\(65\)90153-X](https://doi.org/10.1016/0032-3950(65)90153-X).
 - [39] S.D. Stefanidis, S.A. Karakoulia, K.G. Kalogiannis, E.F. Iliopoulou, A. Delimitis, H. Yiannoulakis, T. Zampetakis, A.A. Lappas, K.S. Triantafyllidis, Natural magnesium oxide (MgO) catalysts: a cost-effective sustainable alternative to acid zeolites for the in situ upgrading of biomass fast pyrolysis oil, *Appl. Catal. B Environ.* 196 (2016) 155–173, <https://doi.org/10.1016/j.apcatb.2016.05.031>.
 - [40] K.G. Kalogiannis, S.D. Stefanidis, S.A. Karakoulia, K.S. Triantafyllidis, H. Yiannoulakis, C. Michailof, A.A. Lappas, First pilot scale study of basic vs acidic catalysts in biomass pyrolysis: deoxygenation mechanisms and catalyst deactivation, *Appl. Catal. B Environ.* 238 (2018) 346–357, <https://doi.org/10.1016/j.apcatb.2018.07.016>.
 - [41] M.D. Yuniati, F.C.M.P. Wawuru, A.T. Mursito, I. Setiawan, L. Lintjewas, The characteristics of padamarang magnesite under calcination and hydrothermal treatment, *Ris. Geol. Dan. Pertamb.* 29 (2019), <https://doi.org/10.14203/risetgeotam2019.v29.1016>.
 - [42] A.A. Silva, A.M.F. Sousa, C.R.G. Furtado, N.M.F. Carvalho, Green magnesium oxide prepared by plant extracts: synthesis, properties and applications, *Mater. Today Sustain.* 20 (2022) 100203, <https://doi.org/10.1016/j.mtsust.2022.100203>.
 - [43] P.-A. Deyris, F. Pelissier, C.M. Grison, P. Hesemann, E. Petit, C. Grison, Efficient removal of persistent and emerging organic pollutants by biosorption using abundant biomass wastes, *Chemosphere* 313 (2023) 137307, <https://doi.org/10.1016/j.chemosphere.2022.137307>.
 - [44] D. Laurencin, C. Gervais, H. Stork, S. Krämer, D. Massiot, F. Fayon, ²⁵Mg solid-state NMR of magnesium phosphates: high magnetic field experiments and density functional theory calculations, *J. Phys. Chem. C*. 116 (2012) 19984–19995, <https://doi.org/10.1021/jp307456m>.
 - [45] M.J. Frisch, G.W. Trucks, H.B. Schlegel, G.E. Scuseria, M.A. Robb, J.R. Cheeseman, G. Scalmani, V. Barone, G.A. Petersson, H. Nakatsuji, X. Li, M. Caricato, A.V. Marenich, J. Bloino, B.G. Janesko, R. Gomperts, B. Mennucci, H.P. Hratchian, J.V. Ortiz, A.F. Izmaylov, J.L. Sonnenberg, Williams, F. Ding, F. Lipparini, F. Egidi, J. Goings, B. Peng, A. Petrone, T. Henderson, D. Ranasinghe, V.G. Zakrzewski, J. Gao, N. Rega, G. Zheng, W. Liang, M. Hada, M. Ehara, K. Toyota, R. Fukuda, J. Hasegawa, M. Ishida, T. Nakajima, Y. Honda, O. Kitao, H. Nakai, T. Vreven, K. Throssell, J.A. Montgomery Jr., J.E. Peralta, F. Ogliaro, M.J. Bearpark, J.J. Heyd, E.N. Brothers, K.N. Kudin, V.N. Staroverov, T.A. Keith, R. Kobayashi, J. Normand, K. Raghavachari, A.P. Rendell, J.C. Burant, S.S. Iyengar, J. Tomasi, M. Cossi, J.M. Millam, M. Klene, C. Adamo, R. Cammi, J.W. Ochterski, R.L. Martin, K. Morokuma, O. Farkas, J.B. Foresman, D.J. Fox, *Gaussian 16 Rev. C.01*, (2016).
 - [46] J.E. Kogel, *Industrial Minerals & Rocks: Commodities, Markets, and Uses*, SME, 2006.